LETTER

Efficient Green Solar Cells via a Chemically Polymerizable Donor−Acceptor Heterocyclic Pentamer

Jegadesan Subbiah,[†] Pierre M. Beaujuge,[‡] Kaushik Roy Choudhury,[†] Stefan Ellinger,[‡] John R. Reynolds,*[,‡] and Franky So*[,†]

Department of Materials Science and Engineering and The George and Josephine Butler Polymer Research Laboratory, Department of Chemistry, Center for Macromolecular Science and Engineering, University of Florida, Gainesville, Florida 32611

ABSTRACT In this contribution, we report on bulk-heterojunction solar cells using a solution-processable neutral green conjugated copolymer based on 3,4-dioxythiophene and 2,1,3-benzothiadiazole as the donor and [6,6]phenyl-C61 butyric acid methyl ester (PCBM) as the acceptor. We have found that the short-circuit current is very sensitive to the composition of the donor−acceptor blend and it increases with increasing acceptor concentration. The device with a donor−acceptor ratio of 1:8 gives the best performance with a short-circuit current of 5.56 mA/cm^2, an open-circuit voltage of 0.77 V, and a power conversion efficiency of 1.9% under AM 1.5 solar illumination. The incident photon-to-current efficiency (IPCE) of the green solar cells shows two bands, one with a maximum of 57% in the UV region corresponding to absorption of PCBM and a second one with a maximum of 42% at longer wavelengths corresponding to the absorption of the green polymer.

KEYWORDS: green solar cell • donor−acceptor • bulk heterojunction • conjugated polymers • low band gap

Because of the fast-rising demand for alternative energies, solar power conversion has become a mainstay of research and development. Polymer solar cells (PSCs) (1) are attractive for the next-generation photovoltaics because of their compatibility with flexible substrates and their potential for low manufacturing costs and large area applications (2). To date, bulk-heterojunction (BHJ) PSCs based on interpenetrating networks of semiconducting polymers and fullerene derivatives (3) have shown the best performance with state-of-the-art power conversion efficiencies exceeding 5% (4−7). Taking advantage of the large increase of the interface area between electron-rich and -deficient phases compared to donor−acceptor bilayer heterojunctions, BHJs aim at promoting charge generation across the active layer while maintaining efficient diffusion and subsequent dissociation of photogenerated excitons, allowing the charge carriers to migrate toward the collection electrodes. To enhance the photovoltaic performance, it is desirable to have a low-band-gap polymer with a low-lying highest occupied molecular orbital (HOMO) energy to increase the open-circuit voltage, along with a low-lying lowest unoccupied molecular orbital (LUMO) energy [0.2−0.3 eV from that of [6,6]phenyl-C61 butyric acid methyl ester (PCBM)] to maintain a narrow energy gap. To this end, low-band-gap polymers have been synthesized (5, 8−12) based on the donor−acceptor approach (13).

With band-gap engineering, color tuning in π-conjugated polymers is desirable for photovoltaic applications such as power-generating ornaments or light-harvesting windows where colors are required. While most established high-performance photovoltaic polymers are orange [e.g., poly[2-methoxy-5-(3,7-dimethyloctyloxy)-1,4-phenylenevinylene] (MDMO-PPV)] (14), red [e.g., poly(3-hexylthiophene) (P3HT)] (15), or blue [e.g., poly[2,6-[4,4-bis(2-ethylhexyl)-4*H*-cyclopenta[2,1-*b*;3,4-*b*′]dithiophene]-*alt*-4,7-(2,1,3-benzothiadiazole)]] (16) in devices, only a few recent reports have described the use of green polymers in PSCs (9, 17). In parallel, dye-sensitized solar cells of practically any color have been reported based on the use of small molecules (18−20). Herein, we report on the photovoltaic performance of a neutral-state saturated green π-conjugated polymer specifically designed to combine both excellent charge-transport properties and a two-band absorption across the visible spectrum for light-harvesting. The proposed synthetic design is highly versatile, hence opening the doors to further structural modifications and solar cell performance enhancement.

As demonstrated by various groups, the color green is not readily accessible in π-conjugated polymers and the polymer backbone has to be carefully designed to provide a two-band optical absorption in the visible region of the electromagnetic spectrum centered with a window of transmission in the 490−560-nm range (21−23). While exploring the use of the donor−acceptor approach in the design of novel soluble electrochromic polymers reflecting and/or transmitting color

* To whom correspondence should be addressed. E-mail: reynolds@chem.ufl.edu (J.R.R.), fso@mse.ufl.edu (F.S.).
Received for review February 22, 2009 and accepted April 28, 2009
† Department of Materials Science and Engineering.
‡ The George and Josephine Butler Polymer Research Laboratory, Department of Chemistry, Center for Macromolecular Science and Engineering.
DOI: 10.1021/am900116p

Published on Web 05/28/2009

states commonly difficult to achieve, Beaujuge et al. have recently shown that various tones of green could be attained on the sole basis of a linear combination of well-chosen electron-rich and -poor heterocycles (23). In a separate study (24), the same group has further described how the short- and long-wavelength absorption bands could be adjusted in terms of their relative intensities and overlap by varying the relative contribution of electron-rich and -poor moieties incorporated in the polymer repeat unit. Throughout both studies, a synthetic design relying on the symmetrical functionalization of the acceptor 2,1,3-benzothiadiazole (BTD) with different alkyl-substituted and unsubstituted thienylene donors afforded oligomers exhibiting especially low oxidation potentials, which could subsequently be oxidatively polymerized using mild conditions. While these materials were designed to be spray-processed as electrochromic thin films for display applications, they do not commonly show any particular propensity to order or π-stack in the solid state because of the large number of solubilizing side chains incorporated (25, 26). Pendant groups usually affect the overall planarity (27−29), structural arrangement (30), and intermolecular interactions (31) of the polymer backbones, altering charge-transport properties (32−35) and the performance in photovoltaic devices (36, 37).

As illustrated in Figure 1a, we have now designed a repeat unit retaining the polymer two-band absorption in the visible required to set the color green by first symmetrically substituting two electron-rich 3,4-dialkoxythiophenes (DalkOTs) onto BTD using Stille conditions (38). The DalkOTs were next functionalized with unsubstituted thiophene rings, affording a symmetrical donor−acceptor pentamer, the oxidative polymerization of which resulted in a coplanar bithiophene bridge regularly spacing the DalkOTs along the backbone of the polymer, namely, PGREEN. As previously described, it is expected that lowering the concentration of solubilizing groups to the necessary extent reduces the chain-to-chain distances (or lamellar spacing) and promotes π-stacking interactions (39−41).

As shown in Figure 1b, PGREEN exhibited the anticipated two-band absorption features both in solution (toluene here) and in the solid state. Importantly, PGREEN is perceived as green in color as a film where the 25-nm red shift of the transmission window was sufficient to yield the desired color. In contrast, without the presence of the bithienyl coplanar spacer, the resulting polymer was blue in solution as well as in the solid state, as first described by Janssen et al. (42). Determined from the onset of its lowest energy transition (750 nm), PGREEN exhibits a relatively low band gap of 1.65 eV. In solution, PGREEN shows only minor optical changes upon elevation of the temperature between room temperature and 100 °C, supporting the absence of any significant aggregation (43, 44) or disruption of the solvated conjugated backbones (45, 46). Films of PGREEN were cast onto a platinum button electrode from room temperature toluene and subsequently redox-cycled in a 0.1 M TBAP/propylene carbonate electrolyte solution (in an argon-filled glovebox) until they reached a stable and reproducible switch prior to electrochemical analysis. The oxidation and reduction potentials of the polymer were investigated by cyclic voltammetry (CV) and differential pulse voltammetry (DPV). Figure 1c describes the redox process undergone by the polymer upon progressive electrochemical doping monitored by DPV, which commonly provides sharper redox onsets than CV when investigating π-conjugated polymers (47). The low oxidation potential of the polymer (+0.43 V by DPV and +0.5 V by CV vs Fc/Fc^+) and its onset of reduction (−1.47 V by DPV and −1.6 V by CV vs Fc/Fc^+) were used to calculate the HOMO (5.53 eV vs

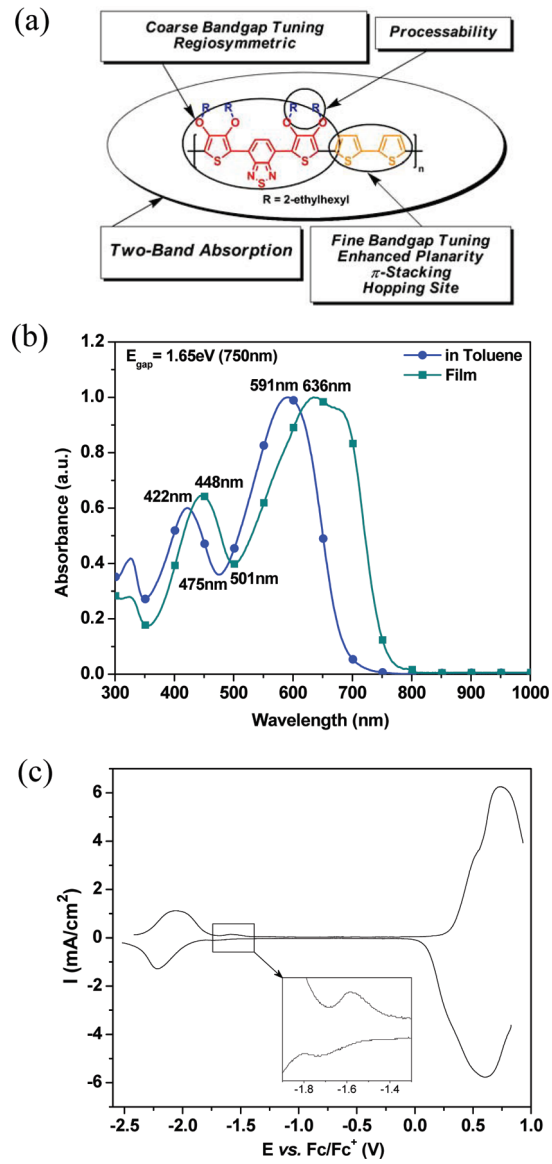

FIGURE 1. (a) Schematic design of donor−acceptor heterocyclic polymers via polymerizable pentamers to yield processable neutral-state green polymers suitable for photovoltaic applications. (b) Solution and thin-film optical absorption spectra of PGREEN (spectra normalized at the longer-wavelength absorption maximum). (c) DPV characterization of PGREEN cast onto a platinum button electrode. The experiment was carried out under an argon atmosphere, in a 0.1 M TBAP/propylene carbonate electrolyte solution, using a platinum flag as the counter electrode and a silver wire as the reference electrode (which was then referenced vs Fc/Fc^+). The inset emphasizes the first reduction process monitored in the negative potential range.

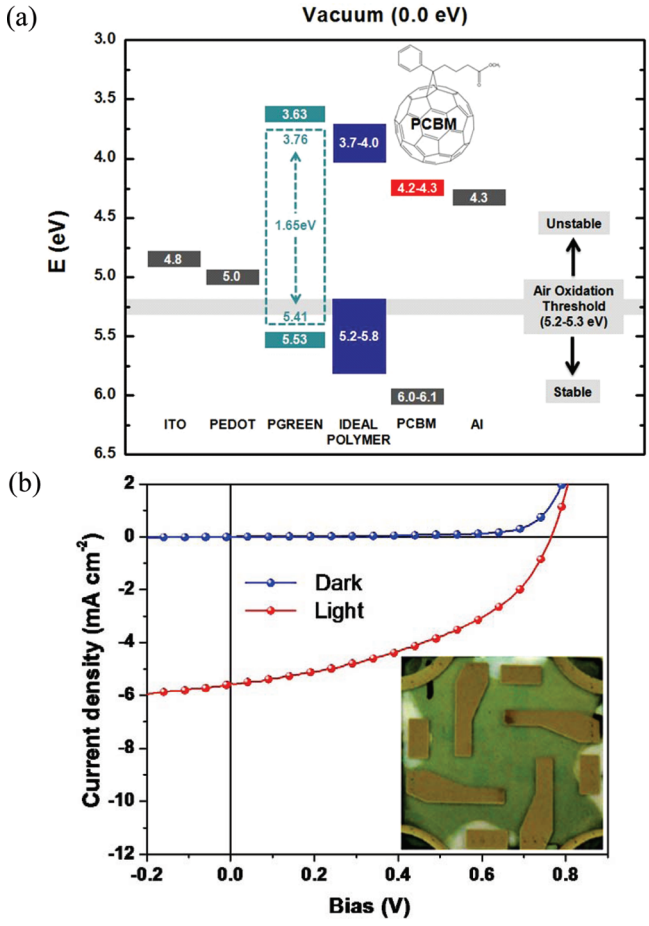

FIGURE 2. (a) Energy-level diagram for PGREEN as estimated by DPV (green filled rectangles) relative to those of an "ideal polymer" (designed for use with PCBM and PEDOT in BHJ solar cells). The optically determined band gap was placed at the baricenter of the electrochemical band gap, and a second approximated set of HOMO and LUMO levels could be defined, assuming the energy levels equidistant from the baricenter (in a green dotted rectangle). (b) $I-V$ curves of a PGREEN-based BHJ solar cell (PGREEN:PCBM = 1:8) in the dark (blue) and under illumination of AM 1.5G, 100 mW/cm^2 (red). The photograph illustrates the green hue attained at the corresponding PGREEN/PCBM ratio (1:8).

vacuum) and LUMO (3.63 eV vs vacuum) levels of PGREEN [$E_{HOMO} = E_{OX}$(DPV) + 5.1 eV and $E_{LUMO} = E_{RED}$(DPV) + 5.1 eV]. The corresponding electrochemically determined band gap of 1.9 eV differs from the optically estimated gap (1.65 eV) by 0.35 eV. Such differences between electrochemically and optically estimated values in donor−acceptor polymers have been reported in work from various groups (48−50). The signal corresponding to the first reduction process observed was relatively weak (see the inset of Figure 1c) in comparison to that of the second reduction process observed, which induced the degradation of the polymer on repeated cycling. The onset of reduction measured from the first reduction process is in good agreement with the literature for donor−acceptor polymers containing BTD (16, 51, 52). The DPV-estimated energy levels of the polymer were used to construct the energy diagram depicted in Figure 2a, which demonstrates the band structure of the polymer with respect to the different variables conventionally involved in organic solar cell development (4, 16). In particular, the polymer's relatively deep HOMO level should induce a favorable

Table 1. PSC Device Performance as a Function of the PGREEN/PCBM Blend Ratio

PGREEN/PCBM ratio (by weight)	J_{sc} (mA/cm^2)	V_{oc} (V)	FF	PCE (%)
1:4	1.99	0.78	0.41	0.64
1:6	3.93	0.77	0.46	1.39
1:7	4.79	0.76	0.46	1.68
1:8	5.56	0.77	0.44	1.90
1:9	3.97	0.73	0.35	1.00
1:10	2.10	0.71	0.40	0.60

increase of the open-circuit voltage and hence the solar cell power conversion efficiency (PCE) (1, 2).

BHJ photovoltaic cells (Figure S3 in the Supporting Information) were fabricated using PGREEN as the donor and PCBM as the acceptor. Their photovoltaic characteristics are shown in Figure 2b. First, the PGREEN/PCBM blend composition was optimized by characterizing the device performance as a function of the composition. Table 1 shows the photovoltaic performance of a series of devices fabricated with different PCBM loadings, and Figure 2b shows the current density−voltage ($J-V$) characteristics of a device made with an optimized donor−acceptor ratio of 1:8. From Table 1, it can be seen that the short-circuit current (J_{sc}) increases with increasing PCBM content in the devices and reaches a maximum value of 5.56 mA/cm^2 when the blend ratio is 1:8 (see Figure S2 in the Supporting Information). Both the open-circuit voltage (V_{oc}) and the fill factor (FF) of this device are 0.77 V and 45%, respectively. At this optimized blend ratio, the device shows 1.9% power conversion efficiency (PCE). Further increase of the PCBM content lowers the short-circuit current (see Figure S2 in the Supporting Information). These results show that the performance of the solar cells fabricated with PGREEN is sensitive to the amount of PCBM incorporated. It has been demonstrated for photovoltaic cells using relatively disordered polymers, such as MDMO-PPV, that the optimum device performance is commonly obtained with a donor−acceptor ratio of 1:4 (53). Because PCBM contributes only minimally to the overall visible light absorption of the blend, increasing its concentration to such a high extent in the cells studied here was not expected to improve the device performance. In principle, higher donor concentrations are desired to improve solar photon flux absorption. However, van Duren et al. reported that, in addition to efficient light absorption, the morphology of the active layer and its organization at the nanoscale is a critical factor determining the device performance (54). In MDMO-PPV/PCBM photovoltaic cells, it has been shown that both the electron and hole mobilities increase with increasing PCBM loading and saturate at 80 wt %. In fact, the hole mobility of the MDMO-PPV/PCBM blend is more than 2 orders of magnitude higher than that of the neat MDMO-PPV film (55). The low hole mobility in neat MDMO-PPV films has been attributed to the formation of interconnected ringlike bent polymer chains and the weakly ordered stacking. It has been proposed that, upon blending with PCBM, the MDMO-PPV chains become fully

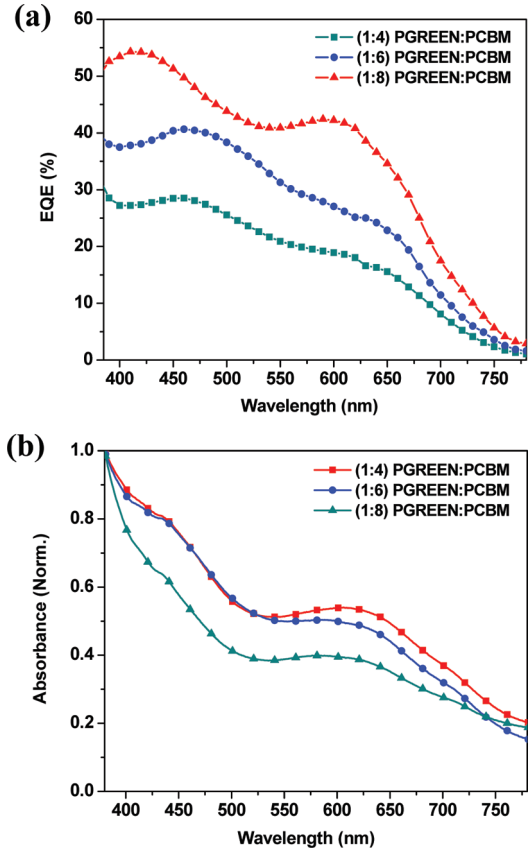

FIGURE 3. (a) EQE for PGREEN/PCBM BHJ photovoltaic devices as a function of the PGREEN/PCBM composition (1:4, 1:6, and 1:8). (b) Normalized optical absorption spectra of the corresponding blends in the same devices.

extended, resulting in enhanced hole transport (55) and photovoltaic device performance.

The external quantum efficiencies (EQEs) of the PGREEN/PCBM devices with the donor–acceptor ratios of 1:4, 1:6, and 1:8 are shown in Figure 3a. Two broad responses are evident with the long-wavelength band attributed to absorption of the polymer and the shorter-wavelength band to absorption by PCBM. In addition, the onset of the photocurrent at 750 nm is in good agreement with the optical absorption results (see Figure 1b). It is interesting to note that the EQE of the photovoltaic cells with 80% PCBM (blend ratio of 1:4) shows a maximum value of 28% at 460 nm, while the EQE of the device with 88.9% PCBM (blend ratio of 1:8) shows a maximum value of 54% at the same wavelength. To elucidate the origin of the increased EQE with decreasing concentration of PGREEN, we then studied the optical absorption of the PSC with blend ratios of 1:4, 1:6 & 1:8, and the corresponding absorption spectra shown in Figure 3b. Given that there is no substantial difference between the absorption spectra of all of the blends, we attribute the remarkable enhancement in EQE to an increase in the charge-carrier mobility, similar to the MDMO-PPV/PCBM system.

In order to verify the above hypothesis, we studied the effect of the PGREEN/PCBM blend composition on charge transport. To this end, hole-only devices, consisting of a layer of either just the PGREEN polymer or the PGREEN/PCBM blend sandwiched between a PEDOT/PSS-coated indium–tin oxide (ITO) electrode and a palladium counter electrode (56) as the electron-blocking contact, were fabricated. From the current density (J) as a function of the electric field data (Figure S4 in the Supporting Information), the hole mobility in the trap-free space-charge-limited-current (SCLC) region can be estimated using the Mott–Gurney equation for trap-free SCLC: $J = (9/8)\mu\varepsilon(V^2/d^3)$, where ϵ is the dielectric constant, μ is the charge-carrier mobility, d is the sample thickness, and V is the voltage across the sample. The voltage across the sample is obtained by subtracting the built-in voltage from the applied voltage. Using this expression, the hole mobility of the pristine polymer was calculated as 5×10^{-6} cm^2/(V s), which is an order of magnitude higher than that of MDMO-PPV [5×10^{-7} cm^2(V s)] (55). At the optimum blend composition of PGREEN/PCBM (1:8), the hole mobility undergoes an increase by an order of magnitude, reaching 4×10^{-5} cm^2/(V s). These results indicate that higher PCBM content enhances the hole mobility of the active layer in the device in a manner similar to that observed in MDMO-PPV/PCBM-based photovoltaic cells (55), hence facilitating the transport and collection of the positively charged carriers at the anode. In parallel, it is likely that the higher PCBM content in the blend provides an effective percolating pathway of relatively high mobility, as required for rapid electron transport across the active layer and collection at the cathode.

Table 2. PSC Device Performance as a Function of the Active-Layer Film Thickness

thickness (nm)	J_{sc} (mA/cm^2)	V_{oc} (V)	FF	PCE (%)
50	1.71	0.61	0.43	0.45
90	4.80	0.75	0.42	1.50
120	5.56	0.77	0.44	1.90
145	4.52	0.77	0.42	1.46

Though the polymer content in the best device is relatively low (~11%), the absorption of PGREEN remains significant (see Figure 3b) because of the high absorption coefficient of PGREEN (2.2×10^5 cm^{-1} at 642 nm) in comparison to that of P3HT (1.6×10^5 cm^{-1} at 523 nm). In addition to the higher absorption of the polymer, the active-layer thickness plays a determining role in the extent of sunlight absorbed, which is, in turn, reflected by the short-circuit current. Table 2 shows the device performance at various active-layer thicknesses, revealing that the short-circuit current decreases as the film thickness decreases. The optimum device performance was obtained with a film thickness of 120 nm.

In summary, we have described the use of a new π-conjugated donor–acceptor polymer with two-band absorption in the visible that reflects the color green in photovoltaic devices. Our approach offers new perspectives for applications where color tunability is desirable such as aesthetically pleasing solid-state flexible organic solar cells and light-harvesting windows.

Acknowledgment. The authors gratefully acknowledge financial support from Sestar, LLC.

Supporting Information Available: Experimental details, synthesis of **7** and **8**, plots of the variation of the short-circuit current and the efficiency of the green cell, schematic diagram of a photovoltaic device structure, and *I*−*V* curve of the single carrier device. This material is available free of charge via the Internet at http://pubs.acs.org.

REFERENCES AND NOTES

(1) (a) Thompson, B. C.; Fréchet, J. M. J. *Angew. Chem., Int. Ed.* **2008**, *47*, 58–77. (b) Bundgaard, E.; Krebs, F. C. *Sol. Energy Mater. Sol. Cells* **2007**, *91*, 954–985. (c) Kroon, R.; Lenes, M.; Hummelen, J. C.; Blom, P. W. M.; Boer, B. *Polym. Rev.* **2008**, *48*, 531–582.

(2) (a) Gunes, S.; Neugebauer, H.; Sariciftci, N. S. *Chem. Rev.* **2007**, *107*, 1324–1338. (b) Krebs, F. C. *Sol. Energy Mater. Sol. Cells* **2009**, *93*, 394–412. (c) Krebs, F. C. *Sol. Energy Mater. Sol. Cells* **2009**, *93*, 465–475.

(3) Yu, G.; Gao, J.; Hummelen, J. C.; Wudl, F.; Heeger, A. J. *Science* **1995**, *270*, 1789–1791.

(4) Li, G.; Shrotriya, V.; Huang, J. S.; Yao, Y.; Moriarty, T.; Emery, K.; Yang, Y. *Nat. Mater.* **2005**, *4*, 864.

(5) Peet, J.; Kim, J. Y.; Coates, N. E.; Ma, W. L.; Moses, D.; Heeger, A. J.; Bazan, G. C. *Nat. Mater.* **2007**, *6*, 497.

(6) Hou, J.; Chen, H.-Y.; Zhang, S.; Li, G.; Yang, Y. *J. Am. Chem. Soc.* **2008**, *130*, 16144–16145.

(7) Wang, E.; Wang, L.; Lan, L.; Luo, C.; Zhuang, W.; Peng, J.; Cao, Y. *Appl. Phys. Lett.* **2008**, *92*, 033307-3.

(8) Scharber, M. C.; Mühlbacher, D.; Koppe, M.; Denk, P.; Waldauf, C.; Heeger, A. J.; Brabec, C. J. *Adv. Mater.* **2006**, *18*, 789–794.

(9) Zhang, F.; Perzon, E.; Wang, X.; Mammo, W.; Andersson, M. R.; Inganäs, O. *Adv. Funct. Mater.* **2005**, *15*, 745–750.

(10) Wong, W. Y.; Wang, X. Z.; He, Z.; Djurisic, A.; Yip, C. T.; Cheung, K. Y.; Wang, H.; Mak, C. K.; Chan, W. K. *Nat. Mater.* **2007**, *6*, 521.

(11) Shi, C.; Yao, Y.; Yang, Y.; Pei, Q. *J. Am. Chem. Soc.* **2006**, *128*, 8980–8986.

(12) Wienk, M. M.; Turbiez, M.; Gilot, J.; Janssen, R. A. J. *Adv. Mater.* **2008**, *20*, 2556–2560.

(13) Havinga, E. E.; Ten Hoeve, W.; Wynberg, H. *Synth. Met.* **1993**, *55*, 299–306.

(14) Dennler, G.; Sariciftci, N. S. *Proc. IEEE* **2005**, *93*, 1429–1439.

(15) Huang, J.; Li, G.; Yang, Y. *Adv. Mater.* **2008**, *20*, 415–419.

(16) Mühlbacher, D.; Scharber, M.; Morana, M.; Zhu, Z.; Waller, D.; Gaudiana, R.; Brabec, C. *Adv. Mater.* **2006**, *18*, 2884–2889.

(17) (a) Zhang, F.; Mammo, W.; Andersson, L. M.; Admassie, S.; Andersson, M. R.; Inganäs, O. *Adv. Mater.* **2006**, *18*, 2169–2173. (b) Wang, X.; Perzon, E.; Mammo, W.; Oswald, F.; Admassie, S.; Persson, N.; Langa, F.; Andersson, M. R.; Inganäs, O. *J. Mater. Chem.* **2008**, *18*, 5468. (c) Mammo, W.; Admassie, S.; Gadisa, A.; Zhang, F.; Inganäs, O.; Andersson, M. R. *Sol. Energy Mater. Sol. Cells* **2007**, *91*, 1010.

(18) Gratzel, M. *J. Photochem. Photobiol. A* **2004**, *164*, 3.

(19) Gledhill, S. E.; Scott, B.; Gregg, B. A. *J. Mater. Res.* **2005**, *20*, 3167–3179.

(20) Kong, F.-T.; Dai, S.-Y.; Wang, K.-J. *Adv. Optoelectron.* **2007**, 1–13.

(21) Sonmez, G.; Shen, C. K. F.; Rubin, Y.; Wudl, F. *Angew. Chem., Int. Ed.* **2004**, *43*, 1498–1502.

(22) Durmus, A.; Gunbas, G. E.; Camurlu, P.; Toppare, L. *Chem. Commun.* **2007**, 3246−3248.

(23) Beaujuge, P. M.; Ellinger, S.; Reynolds, J. R. *Adv. Mater.* **2008**, *20*, 2772–2776.

(24) Beaujuge, P. M.; Ellinger, S.; Reynolds, J. R. *Nat. Mater.* **2008**, *7*, 795–799.

(25) Campos, L. M.; Mozer, A. J.; Günes, S.; Winder, C.; Neugebauer, H.; Sariciftci, N. S.; Thompson, B. C.; Reeves, B. D.; Grenier, C. R. G.; Reynolds, J. R. *Sol. Energy Mater. Sol. Cells* **2006**, *90*, 3531–3546.

(26) Galand, E. M.; Kim, Y.-G.; Mwaura, J. K.; Jones, A. G.; McCarley, T. D.; Shrotriya, V.; Yang, Y.; Reynolds, J. R. *Macromolecules* **2006**, *39*, 9132–9142.

(27) McCullough, R. D.; Lowe, R. D. *J. Chem. Soc., Chem. Commun.* **1992**, *1*, 70–72.

(28) McCullough, R. D.; Lowe, R. D.; Jayaraman, M.; Anderson, D. L. *J. Org. Chem.* **1993**, *58*, 904–912.

(29) San Miguel, L.; Matzger, A. J. *Macromolecules* **2007**, *40*, 9233–9237.

(30) Prosa, T. J.; Winokur, M. J.; Moulton, J.; Smith, P.; Heeger, A. J. *Macromolecules* **1992**, *25*, 4364–4372.

(31) Boon, K. Y.; Ruidong, X.; Mariano, C.-Q.; Paul, N. S.; Bradley, D. D. C. *Nat. Mater.* **2008**, *7*, 376–380.

(32) McCulloch, I.; Bailey, C.; Giles, M.; Heeney, M.; Love, I.; Shkunov, M.; Sparrowe, D.; Tierney, S. *Chem. Mater.* **2005**, *17*, 1381–1385.

(33) Babel, A.; Jenekhe, S. A. *J. Phys. Chem. B* **2003**, *107*, 1749–1754.

(34) Mitzi, D. B.; Yuan, M.; Liu, W.; Kellock, A. J.; Chey, S. J.; Deline, V.; Schrott, A. G. *Adv. Mater.* **2008**, *20*, 3657–3662.

(35) McCulloch, I.; Heeney, M.; Bailey, C.; Genevicius, K.; MacDonald, I.; Shkunov, M.; Sparrowe, D.; Tierney, S.; Wagner, R.; Zhang, W.; Chabinyc, M. L.; Kline, R. J.; McGehee, M. D.; Toney, M. F. *Nat. Mater.* **2006**, *5*, 328–333.

(36) Li, Y.; Zou, Y. *Adv. Mater.* **2008**, *20*, 2952–2958.

(37) Thompson, B. C.; Kim, B. J.; Kavulak, D. F.; Sivula, K.; Mauldin, C.; Frechet, J. M. J. *Macromolecules* **2007**, *40*, 7425–7428.

(38) John, K. S. *Angew. Chem., Int. Ed.* **1986**, *25*, 508–524.

(39) Osaka, I.; McCullough, R. D. *Acc. Chem. Res.* **2008**, *41*, 1202–1214.

(40) Lu, G.; Usta, H.; Risko, C.; Wang, L.; Facchetti, A.; Ratner, M. A.; Marks, T. J. *J. Am. Chem. Soc.* **2008**, *130*, 7670–7685.

(41) Usta, H.; Lu, G.; Facchetti, A.; Marks, T. J. *J. Am. Chem. Soc.* **2006**, *128*, 9034–9035.

(42) Wienk, M. M.; Struijk, M. P.; Janssen, R. A. J. *Chem. Phys. Lett.* **2006**, *422*, 488–491.

(43) Yue, S.; Berry, G. C.; McCullough, R. D. *Macromolecules* **1996**, *29*, 933–939.

(44) Apperloo, J. J.; Janssen, R. A. J.; Malenfant, P. R. L.; Frechet, J. M. J. *Macromolecules* **2000**, *33*, 7038–7043.

(45) Rughooputh, S. D. D. V.; Hotta, S.; Heeger, A. J.; Wudl, F. *J. Polym. Sci., Part B: Polym. Phys.* **1987**, *25*, 1071–1078.

(46) Faied, K.; Frechette, M.; Ranger, M.; Mazerolle, L.; Levesque, I.; Leclerc, M.; Chen, T.-A.; Rieke, R. D. *Chem. Mater.* **1995**, *7*, 1390–1396.

(47) DuBois, C. J.; Abboud, K. A.; Reynolds, J. R. *J. Phys. Chem. B* **2004**, *108*, 8550–8557.

(48) Thompson, B. C.; Kim, Y.-G.; McCarley, T. D.; Reynolds, J. R. *J. Am. Chem. Soc.* **2006**, *128*, 12714–12725.

(49) Hou, J.; Park, M.-H.; Zhang, S.; Yao, Y.; Chen, L.-M.; Li, J.-H.; Yang, Y. *Macromolecules* **2008**, *41*, 6012–6018.

(50) Hou, J.; Tan, Z.; Yan, Y.; He, Y.; Yang, C.; Li, Y. *J. Am. Chem. Soc.* **2006**, *128*, 4911–4916.

(51) Blouin, N.; Michaud, A.; Gendron, D.; Wakim, S.; Blair, E.; Neagu-Plesu, R.; Belletete, M.; Durocher, G.; Tao, Y.; Leclerc, M. *J. Am. Chem. Soc.* **2008**, *130*, 732–742.

(52) Blouin, N.; Michaud, A.; Leclerc, M. *Adv. Mater.* **2007**, *19*, 2295–2300.

(53) Shaheen, S. E.; Brabec, C. J.; Sariciftci, N. S.; Padinger, F.; Fromherz, T.; Hummelen, J. C. *Appl. Phys. Lett.* **2001**, *78*, 841.

(54) van Duren, J. K. J.; Yang, X.; Loos, J.; Bulle-Lieuwma, C. W. T.; Sieval, A. B.; Hummelen, J. C.; Janssen, R. A. J. *Adv. Funct. Mater.* **2004**, *14*, 425–434.

(55) Melzer, C.; Koop, E. J.; Mihailetchi, V. D.; Blom, P. W. M. *Adv. Funct. Mater.* **2004**, *14*, 865–870.

(56) Mihailetchi, V. D.; Koster, L. J. A.; Blom, P. W. M.; Melzer, C.; de Boer, B.; van Duren, J. K. J.; Janssen, R. A. J. *Adv. Funct. Mater.* **2005**, *15*, 795.

AM900116P